1-1-2021

Quantitative Effects of Electrodialysis Membrane Fouling

John Malone
University of Mississippi

QUANTITATIVE EFFECTS OF ELECTRODIALYSIS MEMBRANE FOULING

A Thesis
presented in partial fulfillment of requirements
for the degree of Master of Science
in the Department of Chemical Engineering
The University of Mississippi

by

JOHN MALONE

December 2021

ABSTRACT

To meet the ever-increasing global demand for fresh water, research is constantly being conducted on separation and purification methods. Electrodialysis (ED) is one of the major technologies that seems able to make significant headway in combatting water shortages. As with all technologies, it is limited by certain aspects, one of those being membrane fouling. This research takes a look at the surprisingly unexamined phenomenon of membrane fouling in ED systems. The ED system studied was tested using conductivity probing, limiting current density analysis, and quartz crystal microbalance with dissipation analysis. Investigation of fouling effects commonly seen in ubiquitous ED systems produced data indicating that fouling increased rather than decreased permeant flux and separation rate, and increased the limiting current density of the system from 23.98 (A/m^2) to 31.43 (A/m^2). A brief explanation is offered for this phenomenon, and future research directions are recommended.

DEDICATION

To whom it concerns.

LIST OF ABBREVIATIONS AND SYMBOLS

AEM	Anion Exchange Membrane
CEM	Cation Exchange Membrane
ED	Electrodialysis
EDI	Electrodeionization
EDR	Electrodialysis Reversal
IEM	Ion Exchange Membrane
LCD	Limiting Current Density
NLGI	National Lubricating Grease Institute
QCM(-D)	Quartz Crystal Microbalance (with Dissipation)
RO	Reverse Osmosis
SA	Sodium Alginate
SDI	Silt Density Index
SM	Spacer Matrix
TDS	Total Dissolved Solids
UPW	Ultrapure Water

ACKNOWLEDGEMENTS

I would like to acknowledge the following notable people I have met in my time at the University of Mississippi. The University of Mississippi Graduate School and my advisor, Dr. Alexander Lopez, for use of his laboratory, equipment, time, guidance, and funding my degree. Dr. Hunain Alkhateb for helping me get reacquainted with quantum mechanics from an engineer's perspective. Dr. John O'Haver for introducing me, not too brutally, to the world of chemical engineering and teaching me to phrase questions and create methods of solution to problems like an engineer. Also, for the random book discussions and for being a library for student book loans. All three of the previous mentioned, thank you for reading this manuscript, enduring my thesis defense, and giving candid feedback. It was greatly appreciated. Dr. Paul Scovazzo for always having his office door open for when I needed a distraction from problem sets, often times his. Andrew Ulmer, whose assistance and data collection has helped get the following results to their current state. Any mistakes or misinterpretations arising from the data fall solely at my feet (unless he did something truly egregious and didn't tell me about it). A special thanks to Levi Petix, for convincing me that usually in scientific endeavors, if everything looks all right, then you're all wrong, and that even though I may know, and you may know – if they just don't have any proof then they're inclined to think it a fabricated misdirection. *Gratias vobis ago*.

TABLE OF CONTENTS

LIST OF TABLES

LIST OF FIGURES

CHAPTER 1: INTRODUCTION

A Brief Introduction to Electrodialysis

Electrodialysis (ED) is a separation technique that uses semipermeable ion exchange membranes (IEMs) to leverage cations' and anions' opposite responses to applied electric potential [1]. Anions will move to an anode; cations will move to a cathode. An anion exchange membrane (AEM) will allow anions to pass, a cation exchange membrane (CEM) will allow cations to pass (Figure 1-1 [1]).

As with other separation methods ED utilizes a driving force to cause separation. In ED systems, this is an applied electric potential gradient. For the applied electric potential to be useful as a driving force, an electrolytic medium must be introduced to allow current flow. An electrolytic medium contains a dissolved electrolyte in solution. A classic example is NaCl dissolved in water, the dissociated sodium and chloride ions being free to move throughout the solution. A moving charge is a current, whether the charge is a bare electron or an ion, so the driving force of applied potential difference is able to attempt to equilibrate through electric current between the two electrodes.

Figure 1-1 shows an electrodialysis cell pair, a CEM paired with an AEM. Industrial electrodialysis systems generally contain many cell pairs in series, called an electrodialysis stack, a diagram of which is shown in Figure 1-2 [2]. Systems studied in research tend to have anywhere from a single IEM to a few cell pairs stacked.

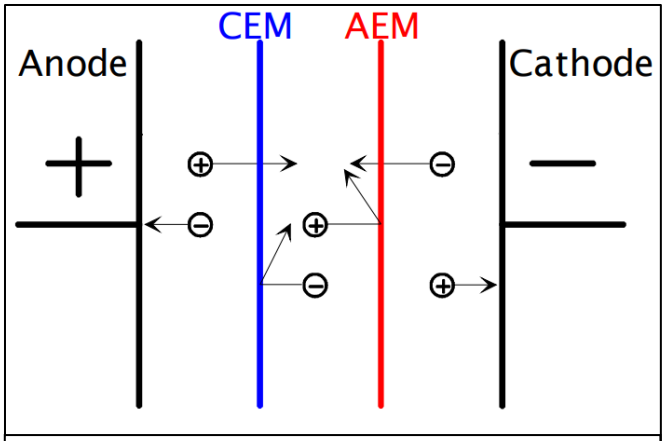

Figure 1-1. Electrodialysis (ED) cell pair diagram.

Ion Exchange Membranes (IEMs) and their Stacking

Ion exchange membranes consist of polymers with charged ligands, the charge type, positive or negative, defining the type of IEM (Figure 1-3 [1]). Separation techniques utilizing IEMs predominantly rely upon charge exclusion of ions. Ions of the same charge type as the membrane are rejected due to electric repulsion. Other factors that influence IEM separation methods are ion valence and diffusion coefficient. As the valence of an ion increases from example X^{-1} to X^{-2}, the repulsion experienced by the ion to the same membrane increases. The diffusion coefficient of an ion will affect how quickly or slowly it passes through the membrane. This is related to several factors, including ion size and sterics.

Cation exchange membranes allow cations to diffuse while blocking anions due to the electronic nature of the negatively charged ligands on the polymer matrix of the membrane (Figure 1-4). Anion exchange membranes perform the same type of separation but allow anions to diffuse while preventing cations from doing so. The charge density of the IEM also plays an important role in the separation efficacy of the system.

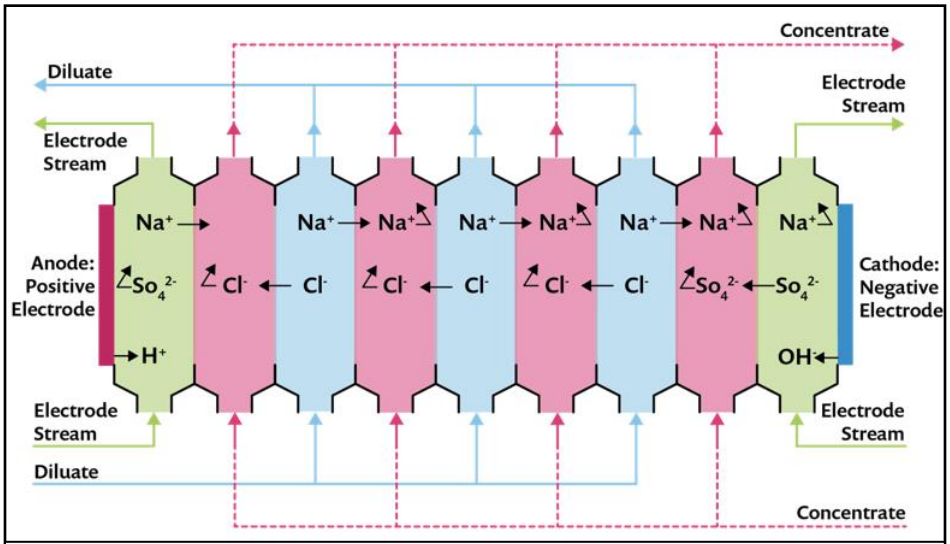

Figure 1-2. Diagram of electrodialysis stack.

Ion exchange membranes tend to swell in water as the high concentration of similar fixed charge ligands experience charge repulsion that is allowed to express once wetted. This swelling is countered by a high degree of polymer crosslinking, which in turn makes the membrane brittle. Because of this IEMs tend to be shipped, stored, and worked with wet. Ion exchange membranes are generally supported by a matrix such as netting or fabric [1].

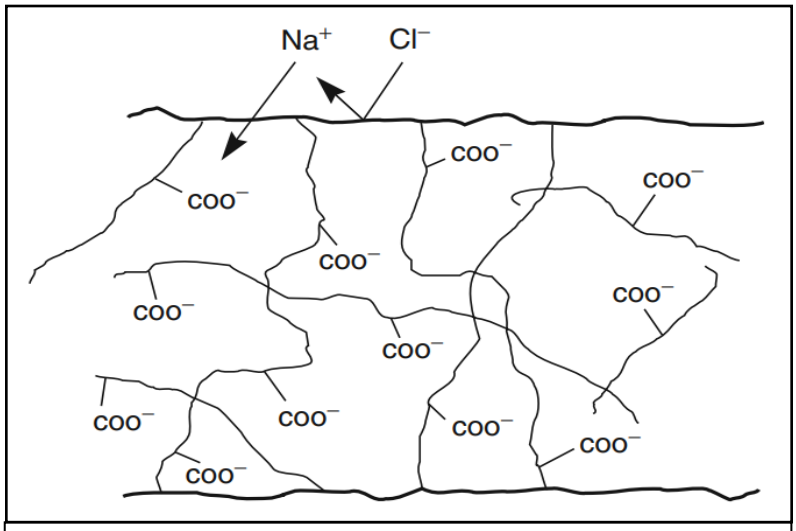

Figure 1-3. CEM polymeric nature with charged ligands.

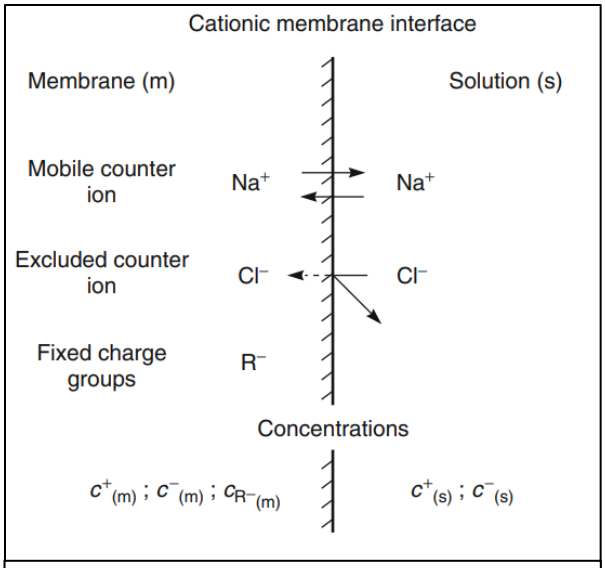

Figure 1-4. Diagram of ion distribution in CEM and surrounding salt solution.

As mentioned above, CEMs and AEMs are paired and grouped as members of a stack. This stacking helps improve the efficiency of ED systems because the same potential difference can be used across many cell pairs, thus causing multiple separation chambers to be affected in concert.

Concentration Polarization

Based on an application of Ohm's Law (V = IR) and idealized electric and concentration gradients (Figure 1-5 [1]), it seems that an ED stack should be able to continuously increase separation and species flux solely by increasing the voltage across the system. Increasing the current of the system would increase the flux of ions, which are separated as they pass through IEMs. Without an appreciable resistance seen anywhere in the system other than in the membranes, and without an increase in resistance, an increased voltage only causes an increased current.

With a perfectly well-mixed electrolyte solution interstitial to the IEMs, essentially no voltage drop would occur in the chambers between the membranes. There would also be a constant bombardment of ions on all faces of all membranes, with separation initiating at the membrane

surface and species fluxing through the ion exchange membranes at their respective rates. As electrodialysis cannot enable separation without bound excepting the applied voltage to the system, there are other factors that need to be accounted for.

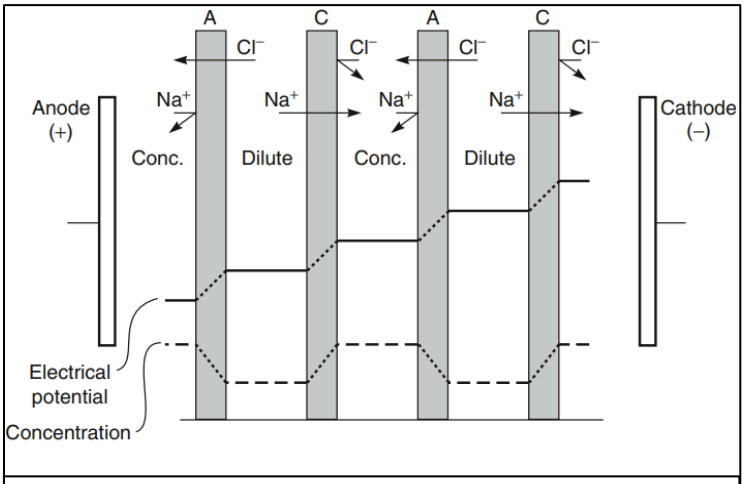

Figure 1-5. Idealized electrodialysis system showing electric potential and concentration gradients.

Concentration polarization accounts for much of the deviation from ideality seen in ED systems. As with all such differences, the result is increased energy expenditure to achieve the theorized separation. Imperfect mixing and system fluid dynamics are the underlying reasons behind concentration polarization. Laminar flow and no-slip conditions at the membrane surfaces create regions of fluid that can be deprived of or enriched with ions in respective chambers. Figure 1-6 shows the effect these regions have on concentration near the membrane surface. In diluate chambers the concentration at the membrane surface is lower than in the bulk of the chamber, and the opposite holds true in the concentrate chambers.

At a given voltage as the concentration of mobile ions near the membrane surface in the diluate chamber decreases, the current will decrease. This follows as a lesser amount of electrolyte in a given volume corresponds to an increased resistance of that volume. More energy is being used to transfer ions across the concentration depleted volume next to the membrane surface. This

correspondence of concentration polarization with increasing intermembrane resistance is shown in Figure 1-7 as a comparison of idealized and non-idealized electric potentials and concentration gradients. The non-idealized potential drops in the chambers, and more in the diluate chambers than concentrate due to the lower concentration of electrolyte.

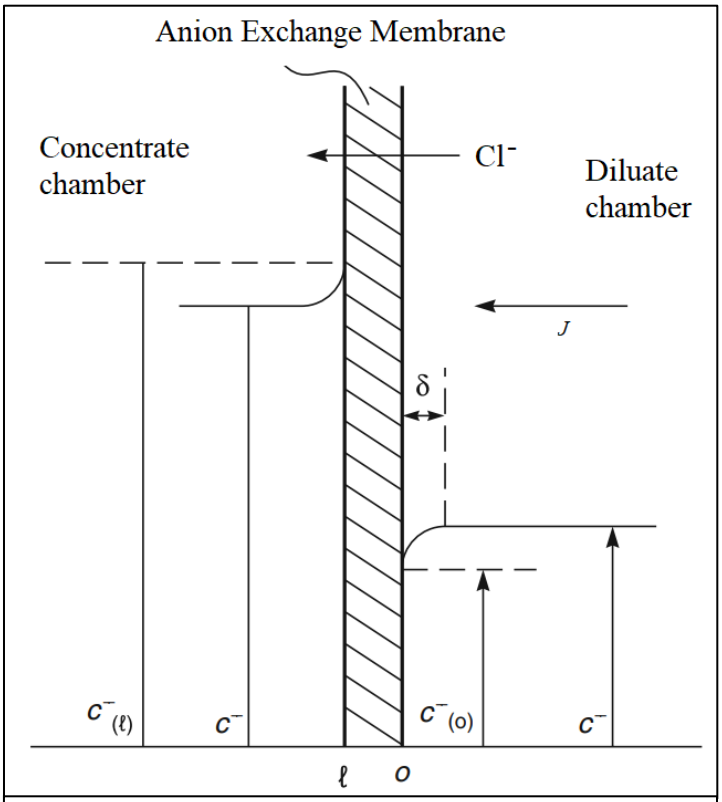

Figure 1-6. Concentration polarization.

The concentration polarization is accentuated by increasing the voltage across the ED stack, as this causes the concentration of ions near the membrane in the diluate chamber to decrease further. This continues until the concentration at the membrane surface is essentially zero, at which point the limiting current of the system has been reached.

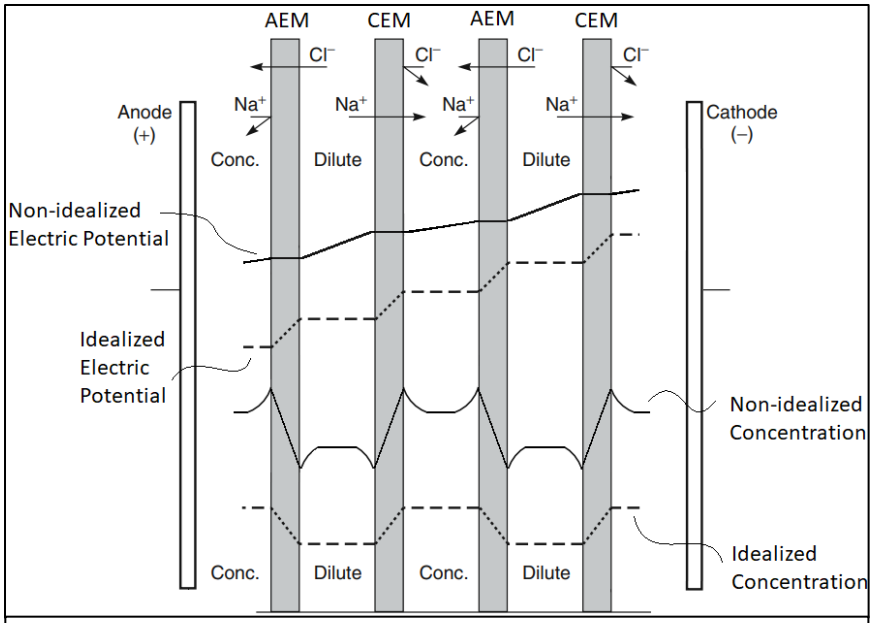

Figure 1-7. Idealized and non-idealized electric potentials and concentration gradients.

Limiting Current Density (LCD)

Once the limiting current has been reached, any increase in voltage will not cause any change in current as there are no more ions capable of transferring charge. Applied voltage over the LCD will generally result in an unregulated flow of ions through all IEMs due to induced electroconvection [3] and, to a small extent, side-reactions such as the electrolysis of water. The limiting current density is that which impacts the efficiency of an ED system.

There are traditionally three electronic regions as applied to ED systems, which are shown in Figure 1-8 [4]. The first is the Ohmic region, in which Ohm's Law holds. In this region, as the voltage across the stack is increased, the current increases proportionally. The Ohmic region ends and the second begins at as the limiting current is reached. This region is the plateau region, in which an increase in voltage has no appreciable increase in current across the stack. The third

region is the over-limiting current region, in which increasing voltage once again increases current. This is the region in which electroconvection and unregulated ion flow occurs [3,4].

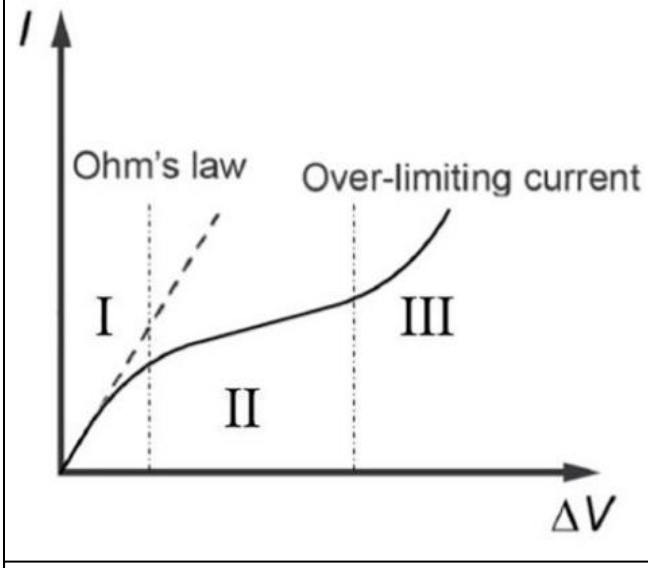

Figure 1-8. Three regions of Ohmic, plateau, and over-limiting current show in I-V graph.

If the LCD is increased, the voltage across the stack can be increased while remaining within the Ohmic region of operation, so the ion transport across membranes increases. This leads to an improved separation time, as voltage has a minimal effect on ED membrane permeance [1]. The actual operating voltage of an ED system is kept well below the LCD threshold, as certain types of fouling can decrease the LCD, thus causing a system to cross into the over-limiting current region, where co-ions and counter-ions pass through both IEMs of the system. Increasing the limiting current density of an ED system is one of the ways to increase the operating efficiency of and electrodialysis system, as it is the main limiting factor of all ED systems.

Fouling

Fouling is a term used to describe the deposition of undesired materials onto a membrane surface during operation. This undesired material typically results in water or ion flux decline within membrane separations due to increased transport resistance [1]. Fouling generally falls into several categories: scale, silt, organic, and biofouling are some examples [1]. All fouling types result in membrane morphology change, be the change surficial or internal. However, fouling that occurs on the surface is more easily addressed through cleaning and backflow operation procedures. Pore clogging and other internal fouling mechanisms require more complex removal procedures to recover separation flux.

Scale, or scaling, is the adsorption of salts precipitated from the feed solution onto a membrane surface. This is commonly seen in desalination processes. The difficulty in reversing scaling depends on the characteristics of salt in the solution. Resolution of scale build-up may be as simple as controlling the pH of the feed or ion exchange through processes such as water softening In essence, antiscalants inhibit the precipitation of salts to the point of keeping traditionally insoluble quantities in solution [5]. Scaling is one of the fouling types most commonly seen in ED systems.

Silt in a separation system is the accumulation of particles on a membrane surface. The buildup of silt incurring flux decline occurs at different rates depending on the silt-particle size and the nominal pore size of a membrane. These effects have been standardized in the silt density index (SDI) of water (ASTM D 4189-95, 2002) [6]. The SDI determines the ability of suspended particles to impair flux by measuring how long a sample takes to pass through a membrane of 0.45 μm pore size at a constant pressure. As the processing time of the sample increases, the rate of plugging/fouling increases and thus so does the SDI value. Not only is this method effective in

predictively bounding how long a filtration process will take, but it also allows for predetermination of the necessity of pretreatment procedures.

Organic fouling is caused by organic compounds adhering to the membrane surface restricting transport and resulting in flux decline. Organic compounds commonly seen with this type of fouling are oils and greases, with greases being more troublesome to deal with [1] (especially as National Lubricating Grease Institute, NLGI, grade increases – becomes harder). This type of fouling may be seen incidentally in local water treatment plants but is more frequently seen in industrial settings where separation occurs to recover solvents or products.

Biofouling is a disparate type of fouling and occurs when bacterial growth begins to inhibit transport. This type of fouling is largely due to the membrane composition, as certain membranes can act as culture plates if the correct conditions are prevalent. This type of fouling is also different in that the fouling itself can degrade the membrane to the point of ruination [1].

While surface fouling is certainly the most common and most readily dealt with, there is also internal membrane fouling, which is the main cause for decreased permeate flux over time [7,8]. This fouling that occurs within the membrane is not necessarily due to an anisotropic nature of the membrane, especially given the anisotropy of contemporary membranes; it is often due to adsorption within the membrane.

There are two genres of dealing with fouling: mitigation and reversal. Fouling mitigation includes feed pretreatment and planned cleaning. Pretreating the feed has the effect of disallowing some types of fouling, such as biofouling, and greatly reducing other types. Biofouling pretreatment generally consists of any steps that will prevent bacterial growth, including bactericides, chlorination, and UV treatment depending on which is least deleterious to the

membrane itself. Organic fouling pretreatment may consist of surfactant treatment, adsorption filtering, an appropriate combination of the two, or ultrafiltration. Silt fouling may be pretreated with the traditional iterative filtration method of continuously decreasing pore-size filtration or depth filtration. It may also be treated with settling tanks or slow filtration if appropriate [9].

Planned cleaning is a maintenance procedure for membranes, the creation of which is often guided by SDI feed results. This procedure is independent of flux decline, though flux is monitored to ensure predetermined levels are met. The cleaning may utilize acidic or alkaline conditions, surfactants, increased pressure, reversed flow, or any combination. The main difference between the two types of fouling mitigation is that pretreatment affects the feed while cleaning affects the membrane itself. In most separation methods scaling is usually dealt with by reverse flushing the membrane with a cleaning solution that is corrosive to the membrane. In ED systems, by reversing the polarity of the electrodes (electrodialysis reversal, EDR), the system will self-descale to a certain degree [10]. This process can be carried out two to four times an hour without appreciable membrane degradation [1]. Indeed, using a proper cleaning regimen, EDR systems have been continuously used in industrial settings without having to change membranes for up to 9 years [3].

While fouling mitigation is essentially passive, fouling reversal is reactive in nature. Once flux drops below a certain threshold, a more vigorous cleaning procedure is followed. As this flux decrease usually coincides with an inadequately pretreated feed, unplanned fouling-induced cleaning usually results in adjustment of pretreatment procedures. When permeate flux is viewed over the time in which cleaning occurs, the benefit of cleaning is apparent, as seen in Figure 1-9 [1].

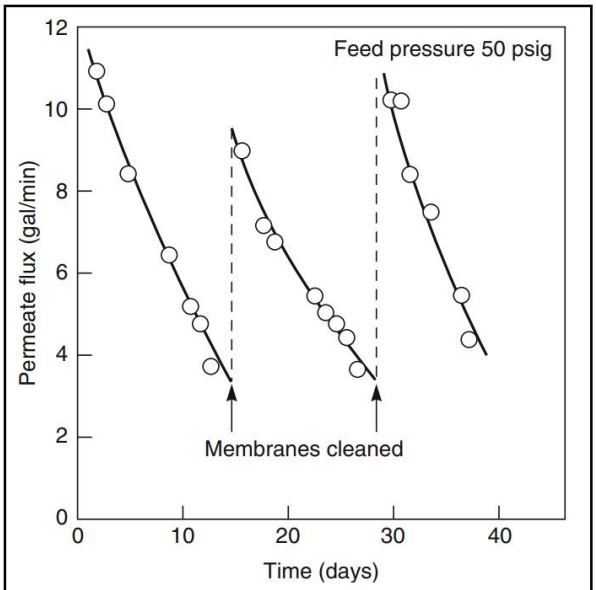

Figure 1-9. Impact of fouling and cleaning on permeate flux over time.

All methods of dealing with fouling are destructive, though the extent varies greatly. Membranes have a certain lifespan that is defined by the flux and permeability degradation of the membrane. This degradation is sped up by cleaning procedures, though planned cleaning is usually accounted for when membrane lifespan is reported [1,3]. Once a certain threshold, predicated mainly on cost relating to flux decline and increase in downtime due to cleaning, is breached, the membrane will be replaced.

Advantages and Disadvantages of Electrodialytic Systems

Several water treatment methods that are currently at the forefront of industrial usage and academic research. These methods can be split into two broad categories, membrane-based and nonmembrane-based [11]. Some of the different methods are listed in Table 1-1.

Table 1-1. Broad categories of separation technologies.

Membrane-based Technologies	Nonmembrane-based Technologies
Electrodialysis (ED)	Distillation
Electrodeionization (EDI)	Flocculation
Reverse Osmosis (RO)	Ion Exchange
Microfiltration/Nanofiltration	Centrifugation

Each of the methods has advantages and disadvantages, and as we are concerned with ED, those shall be enumerated and listed in Table 1-2. The advantages include the energy efficiency within salination feed range, the high level of product purity achievable, the ease of maintenance of a well-developed ED system, that ED is environmentally friendly, the lack of osmotic pressure, and the long system and membrane lifetimes. Disadvantages include decreased energy efficiency at high feed salinity, that ED does not remove uncharged species, the lack of ion selectivity, and membrane fouling [11]. For water with total dissolved solids (TDS) less than 1500 ppm, EDR power consumption is less than that of reverse osmosis (RO) [3], and for TDS <1000 ppm, ED/EDI is favorable to RO as seen in Figure 1-6 [12,13].

One of the main competing separation technologies for creating water of a comparable level of purity as ED/EDI systems is reverse osmosis (RO). While they are both used industrially, research continues to increase the energy efficiency and thus the market share of both. The benefit to a breakthrough in either technology means cheaper clean water, so all advancements are celebrated. That said, there are certain inherent issues with RO systems that ED/EDI systems do not have. Reverse osmosis systems use pressure difference as one of the main driving forces, which creates a host of issues that electric potential gradient does not.

Table 1-2. Advantages and disadvantages of electrodialysis.

Advantages	Disadvantages
Energy efficient within feed salination range	Not energy efficient at high feed salinity
High level of purity	Does not remove uncharged species
Ease of maintenance	Lack of ion selectivity
Environmentally friendly	Membrane fouling
No osmotic pressure	Limiting current
Long system/membrane life	

Keeping a system at pressure is costly, any valve or gasket failure can lead to system failure. Electrodialysis systems can continue separation while the system is leaking, albeit at a decreased efficiency. EDR systems are, to some extent, self-cleaning and can operate with reverse flux if needed, whereas RO systems lack this ability, if only because RO membranes tend to be anisotropic [14].

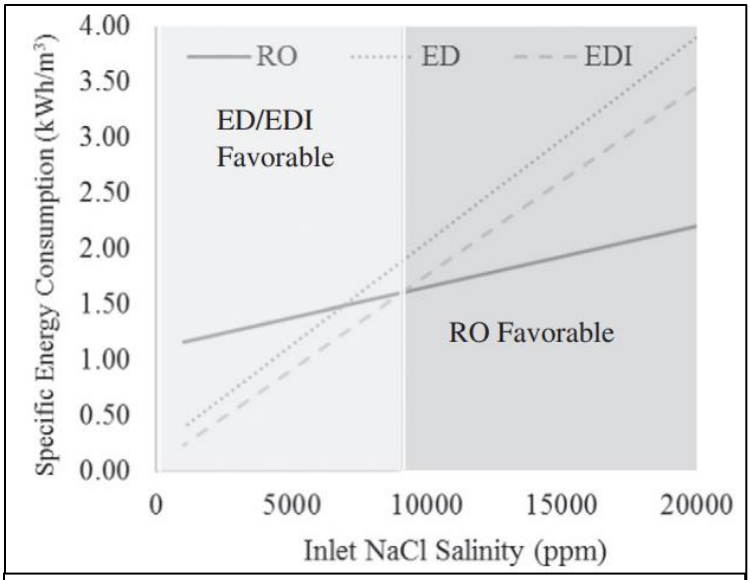

Figure 1-10. Favorability of ED/EDI versus RO.

Perhaps the most notable difference between ED and RO systems is that of approach concentration of salt to the membrane. As discussed, in ED systems the salt concentration approaching the membrane decreases past the bulk concentration until the LCD is reached. In RO systems, the salt concentration approaching the membrane increases past the bulk concentration. This means that RO is inherently bound to encounter scaling issues of some kind. While this has been accounted for in industrial and even home-use systems, scaling remains difficult to address resulting in it remaining the major cause of RO membrane failure [15].

Applications

Purification and separation are often discussed as separate processes, but one cannot exist without the other. The two are omnipresent in modern life, even if they are largely overlooked. As such, many of the applications of ED may be surprising. *Nota bene,* all of the applications mentioned here act on the same basic principles discussed above. Here is a brief account of a few of the current applications of ED systems seen globally.

Since 1892 electrodialysis has been used industrially in the chlor-alkali process [1]. This is the use of a single AEM placed between two electrodes to produce NaOH and Cl_2. By the mid-twentieth century, IEM stacking was suggested, tested, and improved to the point that by 1952 the first ED plant was developed and opened, with several following around the world within the next few years. In the United States, these plants were primarily used for the desalination of water [10].

Contemporary use of ED in plants takes many forms, such as wastewater treatment in the form of salinity reduction; groundwater treatment in the form of nitrate removal, perchlorate reduction, fluoride reduction, and hardness and salts reduction; well water treatment in the form of gas well water desalination; surface water treatment in the form of bromide reduction and

salinity reduction; and uranium mining in the form of sludge desalination [16]. While these constitute many of the major established applications worldwide, there are more specialized uses for ED that are being seen as well. These range from antifreeze and HVAC fluid recycle [17], dairy industry purification [18], and sugar processing [19].

As mentioned, each of these processes uses the same underlying principles, all that changes are the species involved and, in some instances, which stream exists as the desired product. The most striking example of this is seen in Japan, which has no indigenous salt source [20]. Here, ED is used to concentrated salt water, so the concentrate stream (i.e., salt) is the sought product.

All of these processes must use pretreatment procedures to lower the TDS of the feed stream so that the economics of ED are favorable. Understanding the fouling mechanisms that cause flux decrease may lead to breakthroughs that favorably change the robustness and economics of ED systems, allowing for more widespread use of this technology.

CHAPTER 2: EXPERIMENTAL

Materials and Instrumentation

All ED data was gathered using a Masterflex® system. The pump drivers were Masterflex® L/S™ Economy Drive model 07554-90. Masterflex® L/S™ easy-load® II model 77200-62 peristaltic pump heads were used with 24 gauge flexible silicone tubing. The peristaltic pumps were set to a flowrate of 85 rpm (+/- 5 rpm), a rate previously determined to be ideal from previous studies. The stack is housed in a PC Cell 64-4 unit. The stack contains two CEMs and one AEM with spacer matrices (SM) between the IEMs in the configuration: SM, CEM, SM, AEM, SM, CEM, SM. This simplified stack allows for better study of the ED system, especially the AEM. This is useful as it is the anionic portions of the foulants studied that tend to reduce ion flux.

The voltage and current were controlled using a GWinstek GPS-3030DD power supply unit capable of up to 30 volts (+/- 0.1 volts) and 3 amps (+/- 0.01 amps) [21]. All mass measurements were carried out using an Ohaus Adventurer AR240 Analytical Balance with a capacity of 210 g (+/- 0.0001 g). All volumetric measurements were made using the same 1000 mL (+/- 0.3 mL) volumetric flask, 10 mL (+/- 0.02 mL) graduated cylinder, or 100-1000 µL VWR ultra-high performance single-channel pipette (precision +/- 3.3% at 100 µL, +/- 0.8% at 1000 µL, accuracy $\leq$ 0.7% at 100 µL, $\leq$ 0.2% at 1000 µL) where appropriate.

The CEMs used were Neosepta CMX-FG, and the AEMs used were Neosepta AMX-FG. Each membrane sheet was cut into multiple appropriately sized membranes for the Masterflex®

system used. Both membranes are preferentially permselective for ions of the corresponding charge. The type of IEMs used are found in industrial desalination procedures, including those food-grade safe procedures (it can thus be assumed that no deleterious compounds rinse from the neat membranes). The inherent resistance of the CEMs is 1.8 $\Omega * cm^2$ and of the AEMs is 2.6 $\Omega * cm^2$. The nominal CEM thickness is 0.16 mm and the nominal AEM thickness is 0.15mm [22].

The solution used for separation measurements was a simple NaCl and ultrapure water (UPW) solution ranging from 0.01 wt% to 5.00 wt% as indicated. UPW water was collected from a Direct-Q® 3 UV water purification system [23].

The ionicity of these solutions was found by probing with a Thermo Scientific™ Orion™ Dual Star™ pH, ISE, mV, ORP and temperature dual channel benchtop meter before each run and monitored throughout all runs at 5-to-15-minute intervals.

All heating was done using either a Fischerbrand™ Isotemp™ ceramic combination hotplate and stirrer model 11-300-49SHP or an IKA C-MAG HS 7 combination hotplate and stirrer in conjunction with an IKA ETS-D5 electronic contact thermometer.

All quartz crystal microbalance (QCM) testing was done via a Biolin Scientific QSense Analyzer QCM-D system with the included spin coater, and the data were analyzed with the compatible QSense DFind software.

Description of Analytical Procedures

Twenty grams NaCl was dissolved in 1000 mL UPW water to make a 1 wt% solution. This neat NaCl solution was used to find the unfouled flux rate in the ED system. Two 500 mL beakers were filled with 300 mL each of the neat NaCl solution. One was the feed and return respectively for the tubes labeled “diluate in” and “diluate out”, and the other was the feed and return for the

tubes labeled “concentrate in” and “concentrate out” respectively as seen in Figure 2-1. These two beakers, dilute and concentrate, are where the migration of NaCl was measured – from the dilute beaker to the concentrate beaker, both of which start at the same concentration. The flow of each solution is between membranes and is made turbulent despite slow flowrate by sheet flow spacers as seen in Figure 2-2. A potential difference of 3 volts between the two electrodes was held constant for all runs and the amperage was recorded when concentration was. The chloride concentration of the dilute and concentrate beakers was measured and recorded at 15-minute intervals for 180 minutes. This was done three times and the data averaged and error bound as seen in Figures 3-1 and 3-2 as blue circles labeled “neat NaCl”.

Figure 2-1. Photo of ED system used with concentrate and diluate streams labeled.

Next, sodium alginate (SA) was added to the NaCl solution such that it was 0.1 wt% SA. This was then used in place of the neat NaCl previously described. Three runs were again carried out with measurements of both dilute and concentrate beakers made every 15-mintes for 180 minutes. The data was averaged, and error bound as seen in Figure 3-1 as orange squares labeled "0.1 wt% Sodium Alginate". This SA procedure was carried out in the same manner with bovine serum albumin (BSA). The 0.1 wt% BSA data is in Figure 3-1 as grey triangles labeled "0.1 wt% Bovine Serum Alginate".

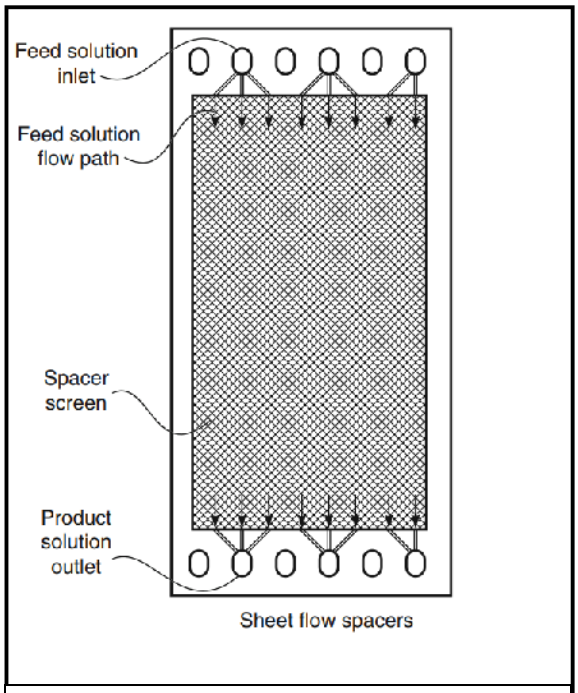

Figure 2-2. Diagram of sheet flow spacer used in ED system.

Abnormal data was recorded in the form of reverse ion transport. As the probe is an old model it was thought that quickly switching between the different concentrations changing in different directions may be compounding any errors. To attempt to negate this introduced error, all further runs were made with the probe in the dilute beaker throughout the runs. While this did

reduce the data available for analysis, the error reduction in the gathered data improved the statistical significance of presented results.

A 0.25 wt% sodium alginate was then run twice with measurements made at the same intervals. The data was averaged and error bound as seen in Figure 3-2 as orange squares labeled "0.25 wt% Sodium Alginate". This procedure then was carried out with a 0.25 wt% bovine serum albumin solution. The BSA data is shown in Figure 3-2 as grey triangles labeled "0.25 wt% Bovine Serum Albumin".

The previously described results are all plotted on the same chart in the Appendix. The data obtained were seemingly anomalous. Whereas the procedure was expected to decrease permeate flux through membranes, data gathered from the system indicated increased permeant flux through the membranes. In an attempt to better understand this, the limiting current density was found. The experimental setup was similar, but a different method was used. Six hundred milliliters of 1 wt% neat NaCl solution were poured into a 1 L beaker. All four concentrate and dilute tubes were placed into the beaker so there would be no net ion transport. This allowed for LCD to be determined by increasing the voltage and amperage (during different runs) of the stack while recycling both the NaCl solution and the Na_2SO_4 solution.

Multiple runs of both neat NaCl and NaCl + SA were made, during which the current was increased every five minutes for three hours and the resulting change in voltage was recorded. The NaCl solution used was 0.05 wt% and the SA was 0.0025 wt% (+/- 1.7%) to ensure the LCD would fall within the restrains of the power supply used. The data were averaged and the LCD was found by submitting it to the graphical regression Cowan-Brown method [4] as seen in Figures 3-4 and 3-5.

Limiting current density data can be used to better understand the system in several ways. It may be used the help obtain correction factors to data-fit equations that model the system using resistance modelling, or it may be used to gain insight into the transport phenomena of the system. Resistance modelling utilizes the same concept behind series resistance seen in circuit and heat transfer analysis. It is shown diagrammatically in Figure 2-3. Each measured resistance of the system is added in series and treated as shown in equation 2-1. Deriving from the general transport equation shown, the flux is treated as contiguous and algebraic, leading to the determination of system resistances as exemplified in equation 2-2.

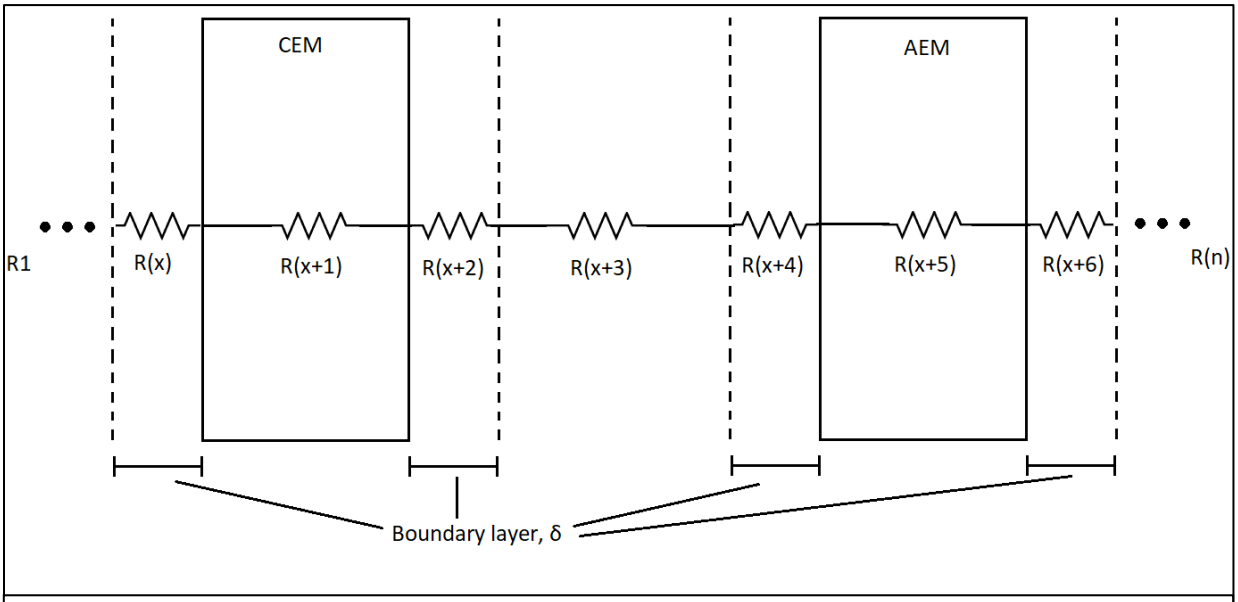

Figure 2-3 Electrodialysis resistance model.

$$J = k\nabla F \rightarrow J_i = k_{net}\left(c_{i_{b,f}} - c_{i_{b,p}}\right) = k_\delta\left(c_{i_{b,f}} - c_{i_{m,o}}\right) = k_m\left(c_{i_{m,o}} - c_{i_{b,p}}\right) \quad \text{2-1}$$

$$1/k_{net} = 1/k_\delta + 1/k_m \quad \text{2-2}$$

These resistances may be defined from data gathered during the experiment, such as volumetric flow rate, $\dot{V}$, diffusion coefficient, *D*, temperature, *T*, and feed channel height, *h*, as shown in equation 2-3. *X* is a coefficient correction factor.

$$k_\delta = X\dot{V}^\alpha h^\beta D^\gamma T^\varepsilon \quad \text{2-3}$$

Using the resistance model provides some insight into the behavior of the system studied, but no extrapolation to other systems may be made, and no insight is gained into the underlying causes of resistance changes.

Treating ED systems with transport-based models allows for deeper understanding of resistance changes. A mathematical treatment of Figure 1-6 leads to the relation between concentrations shown in equation 2-4, allowing a concentration polarization modulus to be defined as in equation 2-5.

$$\left(c_{i,o} - c_{i,p}\right) \Big/ \left(c_{i,b} - c_{i,p}\right) = \exp\left(J\delta \Big/ D\right) \quad \text{2-4}$$

$$E \Big/ E_o = c_{i,p} \Big/ c_{i,o} = \exp\left(J\delta \Big/ D\right) \Big/ \left[1 + E_o\left(\exp\left(J\delta \Big/ D\right)\right) - 1\right] \quad \text{2-5}$$

Equation 2-5 shows that concentration polarization is based on the transmembrane flux, the boundary layer thickness, and the diffusion coefficients. This allows the reasonable postulation that the seemingly anomalous data is a result of a change in one of these factors. Determination of the LCD coupled with the defining limiting current equation (equation 2-6) and the concentration polarization modulus leads to the conclusion that there was a decrease in the boundary layer thickness or the diffusion coefficient, both of which can be determined experimentally.

$$\underset{c_o^- \to 0}{I_{lim}} = {D^- F c^-}/{\delta(1 - t^-)} \quad \text{.....2-6}$$

As the LCD data seemed to agree with the conductivity test data, an experiment was run to try to further quantify the fouling results seen by quartz crystal microbalance with dissipation (QCM-D) testing. A baseline of 2 wt% neat NaCl was run on pristine gold-plated quartz crystal microbalance (QCM) crystals. Then 0.1 wt% SA was added to the solution and run. The same method was used with 0.1 wt% BSA.

To mimic the AEM used in the ED system, an anion exchange ionomer solution (FAA-3-SOLUT-10) from Fumion® was run through the quartz crystal microbalance with dissipation (QCM-D) system onto gold plated QCM crystals for 30 minutes to ensure a buildup of polymerized ionomer [24]. The coated crystals were then used to run neat 2 wt% NaCl and determine any fouling that occurs and if it is easily reversible.

The pristine crystal was normalized with UPW for roughly 12 minutes. Once a baseline was acquired, 0.1 wt% of ionomer solution in UPW was added to the system. This was allowed to run for 30 minutes so an anionic exchange polymer could form, mimicking the AEM used in previous experiments. The system was then rinsed with UPW for 10 minutes to allow any unbound ionomer to be rinsed from the crystal. 2 wt% NaCl solution was added to the system for 20 minutes, mimicking the bombardment of the AEM surface with chloride ions. The system was then rinsed again with UPW for 15 minutes allowing any reversibly bound chloride ions to be washed from the crystal.

CHAPTER 3: RESULTS AND DISCUSSION

Electrodialysis

The expected result from the ED system runs was that added foulant would increase the time for conductivity of the dilute stream to approach zero, which corresponds to a complete removal of chloride from the system. This result could also be seen as lower conductivity of the neat NaCl within a given time frame. As Figure 3-1 shows, contrary to the expected result, the added 0.1 wt% foulants, both SA and BSA, led to a more rapid decrease in conductivity when compared to neat NaCl over the same time. The average difference in concentrations of chloride between the neat NaCl and foulant added solutions were distinct enough to fall outside the standard error bounds of each other.

This was not an isolated occurrence, as the same system was run with a more fouled system of 0.25 wt% SA and BSA with more pronounced results (Figure 3-2). In this run, the BSA caused an extremely noticeable decrease in the conductivity, and thus chloride concentration, of the dilute stream within the first twenty minutes. The data from Figure 3-1 and Figure 3-2 is shown together in the Appendix. It has been reported previously that SA and BSA cause a visible gel layer on the AEM as seen in Figure 3-3 [25].

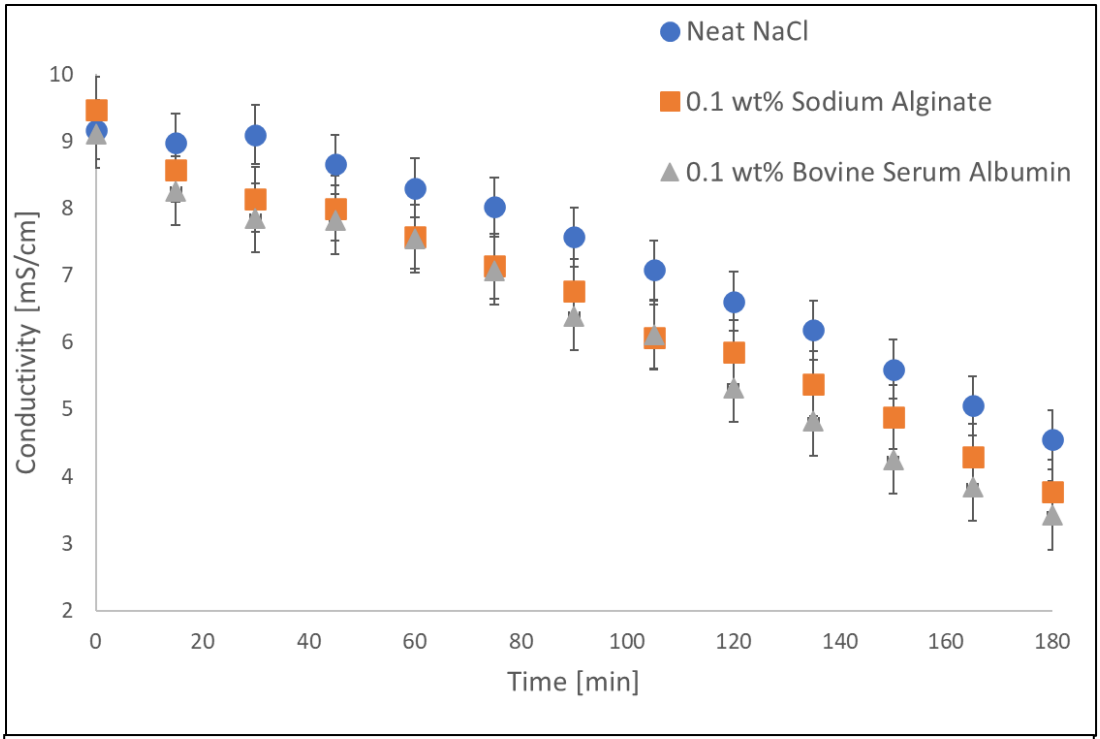

Figure 3-1. Comparison of neat NaCl solution, 0.1 wt% added sodium alginate, 0.1 wt% bovine serum albumin with standard errors.

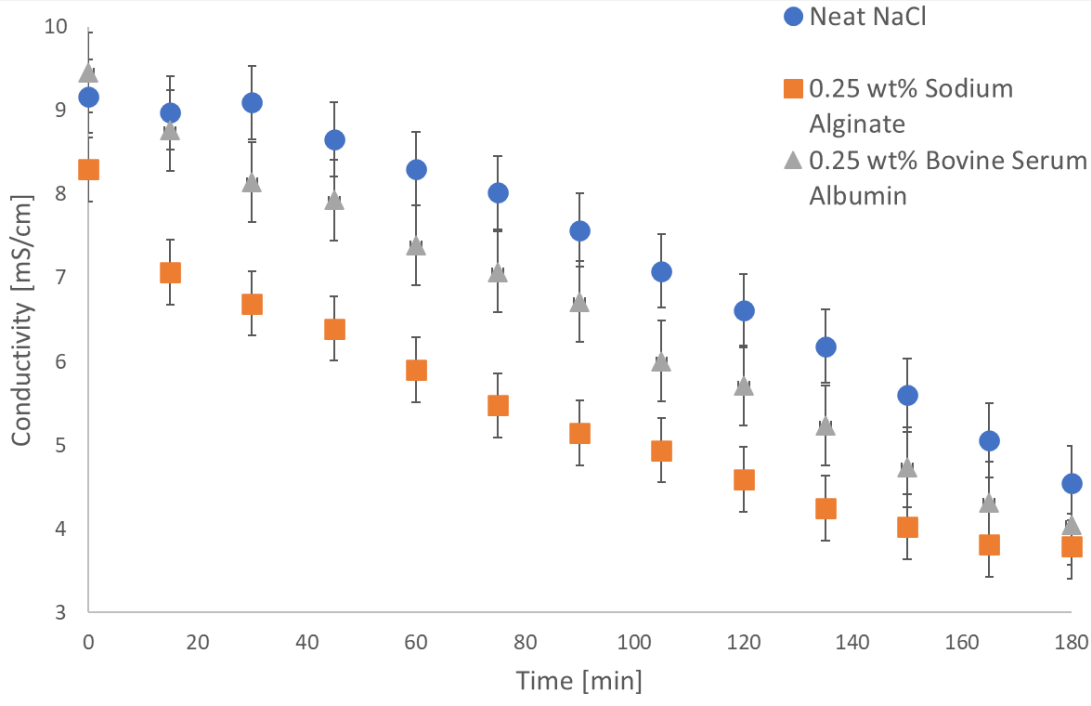

Figure 3-2. Comparison of neat NaCl solution, 0.25 wt% added sodium alginate, 0.25 wt% bovine serum albumin with standard errors.

The unexpected data could have resulted from the formation of a gel layer on the membrane surface where in the neat solution there is only a boundary layer in which a concentration polarization gradient would exist. This new gel layer would have an impact on the boundary layer thickness as well as the concentration polarization gradient magnitude next to the newly expanded membrane interface. Due to the SA and BSA falling out of solution as salts and forming a hydrated gel layer, this new membrane interface is essentially charge neutral. As a result, this lessens the degree of concentration polarization next to the membrane surface for a given voltage across the membrane. To determine if this was occurring, the limiting current density was experimentally determined for neat NaCl solution and NaCl + SA solution.

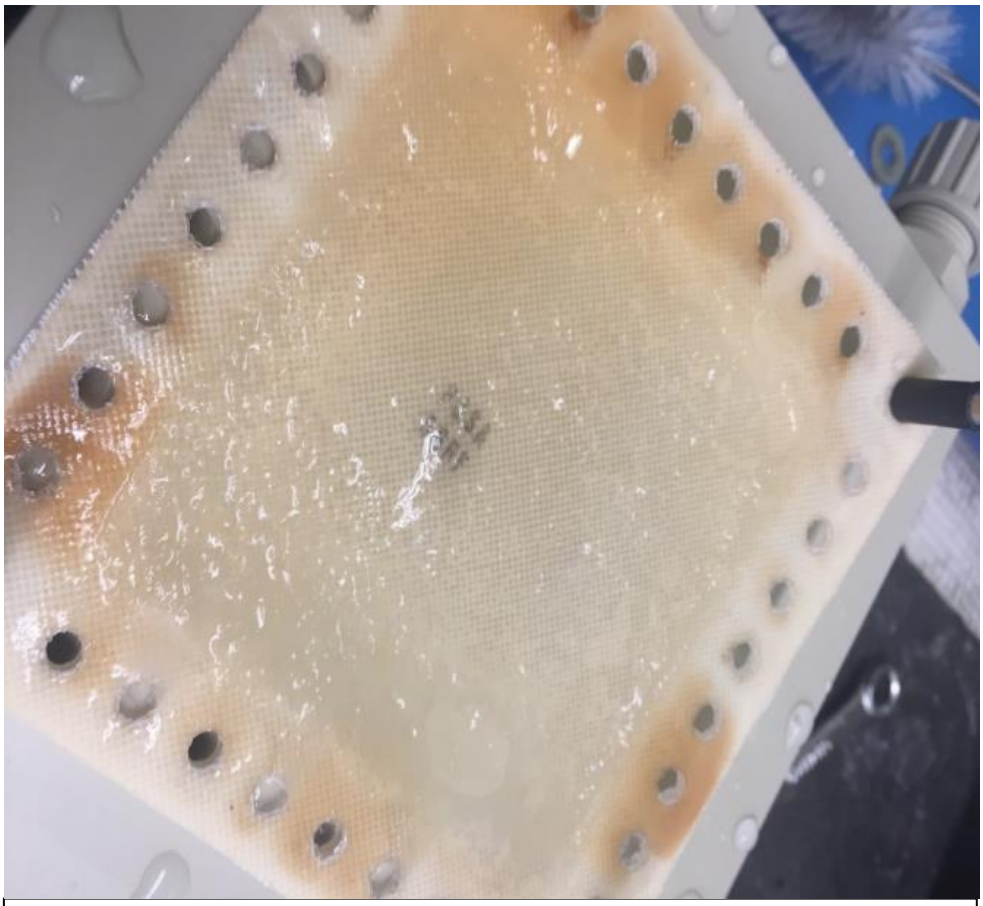

Figure 3-3. Anionic exchange membrane after sodium alginate run [25]

Limiting Current Density

The limiting current density was found experimentally using Cowan-Brown plots of resistance versus LCD^{-1}. Because the graph is nonlinearized through a 1/x transformation, the sensitivity of data analysis is increased in the area needed. Traditional current-voltage graphs were plotted for the data, but the equipment was not sensitive enough to isolate the traditional three regions of Ohmic, limiting current, and over-limiting current shown in Figure 3-4. Many methods of LCD detection use specialized ED systems [26] and electrochemistry-specific devices such as Luggin-Haber capillaries [27].

Figure 3-4 shows the Ω-LC^{-1} graph for neat 0.05 wt% NaCl with linear regressions for the initial and final hyperbolic regions extrapolated past their crossing point. The vertical regression had an R^2 value of 0.9241 and the horizontal regression had an R^2 value of 0.8459. The LCD was determined algebraically from the intersection and found to be 23.98 amps/m^2. The area of the membrane used was 0.0058 m^2 so the limiting current found was 0.14 (+/- 0.01) A. The neat NaCl runs were in very good agreement, with a standard deviation of 0.0002 or 0.71% error (see Appendix for data and analysis).

Figure 3-5 shows the Ω-LC^{-1} graph for 0.0025 wt% (+/- 0.00004 wt%) SA with the same linear regressions performed. Again, it is noted that the concentrations were kept low so as to keep within the limits of the lab power supply, but that the concentration ratio was kept the same as that of the ED experiments. The vertical regression had an R^2 value of 0.9353 and the horizontal regression had an R^2 value of 0.8650. The calculated LCD was 31.43 amps/m^2 and the corresponding limiting current was 0.18 (+/- 0.01) A.

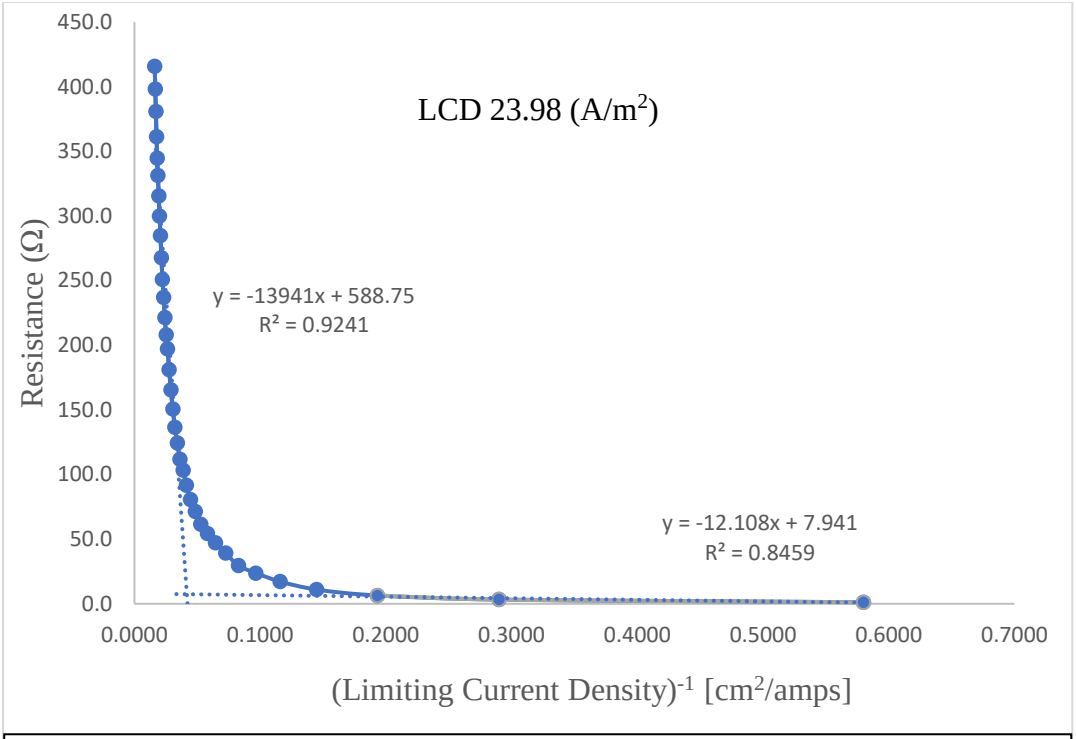

Figure 3-4. Neat NaCl LCD data.

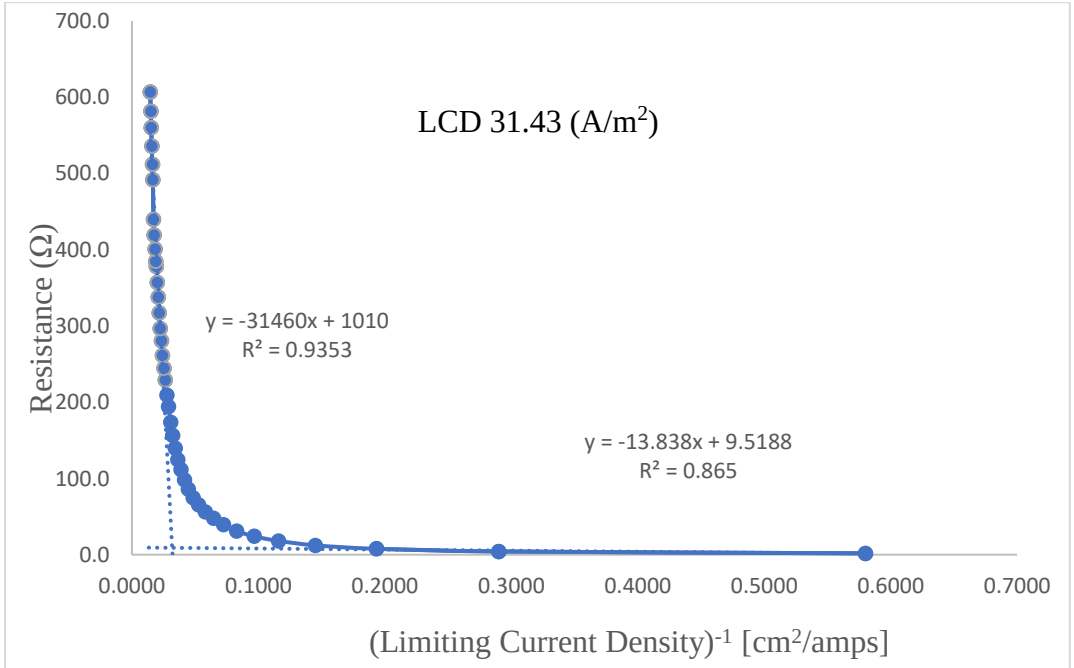

Figure 3-5. 0.0025 wt% sodium alginate LCD data.

Determination of the LCD for neat NaCl and SA fouled ED systems produced results agreeing with those found in the initial ED runs. The addition of foulant increased the LCD of the system. This is rather remarkable as the greater the limiting current density the greater the voltage that can be applied to the system. The increased limiting voltage means a concurrent increase in the acceptable operating voltage and thus an increase in the flux of ions. This may ultimately lead to a decreased time for the same ion transport to occur without sacrificing permeance [3] or membrane selectivity [1]. In other words, adding foulant seems to improve one part of the the operating efficiency of the system [12,13].

Quartz Crystal Microbalance with Dissipation

The presented data indicates that certain foulants can have a beneficial effect on ED systems, though to verify this, the extent of membrane fouling must be quantified and qualified. The impact of fouling on desired ion flux must be accurately measured, and the type of fouling must be determined – reversable or nonreversable. To acquire the data needed, a QCM experiment and analysis were performed.

Figure 3-6 shows the results of the QCM-D experiment. The results are promising as there is clear delineation of mass increase and layer thickness between the addition of different solutions. Some of the effects are due to bulk density differences, however, the horizontal linearity of the plateus indicates that the system is stable.

The increase between the initial thickness and first UPW wash thickness shows the formation of the anion exchange polymer. The second UPW wash also indicates that the NaCl introduced to the system is not permanently fouling the system. This experimental method seems

sound and the results appear to be indicating what is suspected of happening in the ED system. Further experimentation needs to be done.

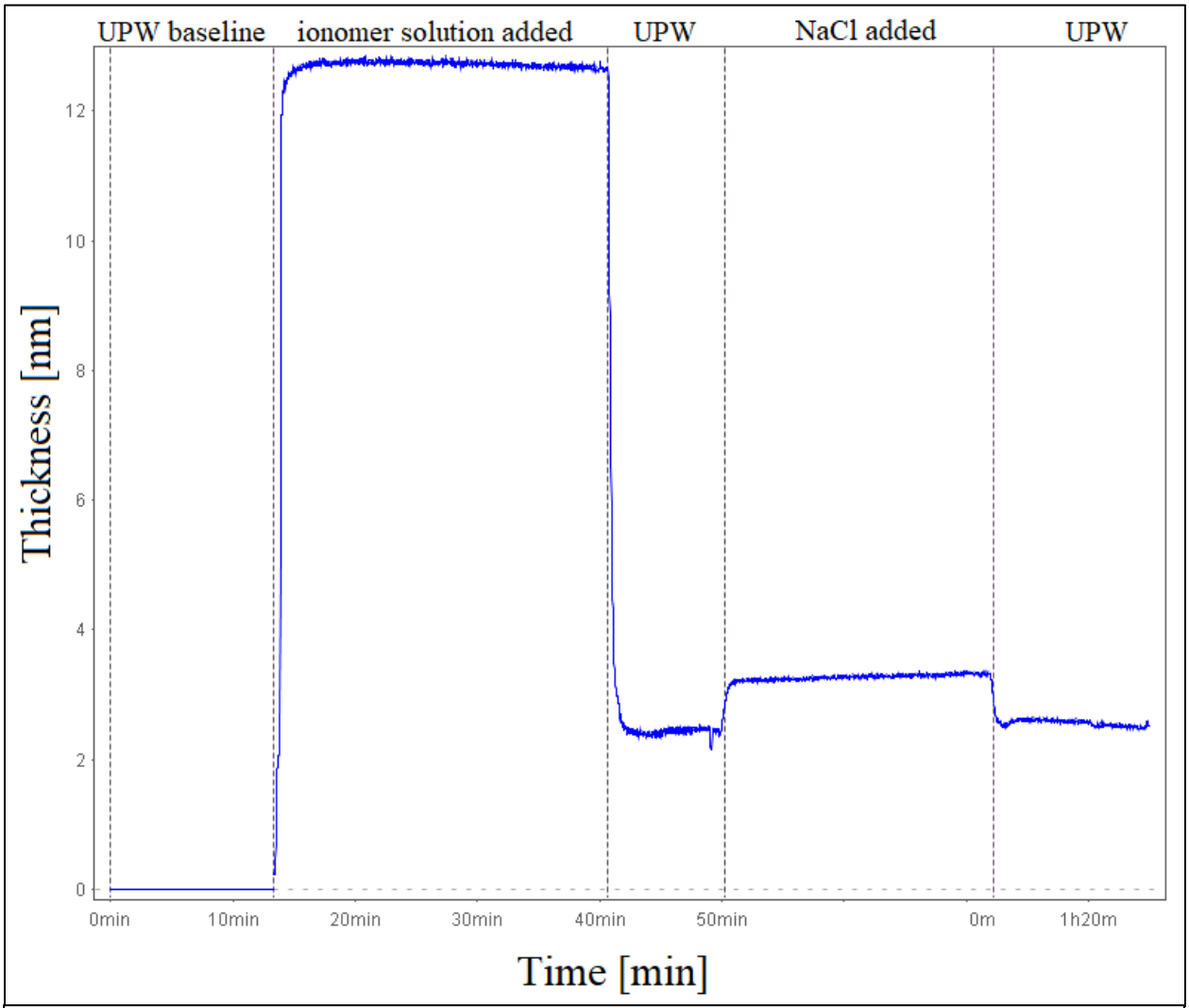

Figure 3-6. QCM thickness data of different solutes added timewise.

CHAPTER 4: CONCLUSIONS AND RECOMMENDATIONS

The ED data shows that organic foulants increase chloride ion flux in the electrodialysis system studied. Both a decrease in the conductivity per unit time of dilute feed and an increase in the LCD with the addition of foulant has been explicitly shown with sound experimental methodology and analysis. The LCD of the system increased by over 31% from 23.98 (A/m^2) to 31.43 (A/m^2). This indicates that ED systems can benefit from foulant inclusion studies regarding their ion transport efficiency, and the optimization of membrane cleaning regimens for separation efficiency.

The QCM data shows excellent results at this stage in the experimental design process. The method shows promise in confirming or refuting the proposed reasoning behind increased chloride flux and LCD, with initial data supporting previous experimental results.

It is recommended that the LCD is determined with bovine serum albumin. A larger data set would be very beneficial, especially as the results were contrary to initial expectations.

It is recommended that the current QCM-D experimental design continues. Study of organic foulants of varying type and concentration ought to be studied. The AEM layer thickness should be increased by increasing run-time or creating multiple runs with UPW rinse between. A cationic ionomer should also be studied. As Ulmer indicated, the current experimental setup allows for testing the efficacy of cleaning methods – both with respect to their overall flux reclamation ability and their time-effectiveness.

It is recommended that electrochemical impedance spectroscopy (EIS) be utilized [24]. A Luggin-Haber system would also be of use. The last recommendation is that a modular ED system be created similar to that found in work done by Krol et al. This would allow more precise resistance and conductivity data to be gathered on individual membranes. Such data would enable identification of concentration polarization influences on both AEM and CEM surfaces.

LIST OF REFERENCES

[1] R.W. Baker, Membrane Technology and Applications, 3rd ed., John Wiley & Sons, Ltd., 2012.

[2] H. Ekström, How to Model Ion-Exchange Membranes and Donnan Potentials, COMSOL. (2018). https://www.comsol.com/blogs/how-to-model-ion-exchange-membranes-and-donnan-potentials/.

[3] Y. Tanaka, Ion Exchange Membranes Fundamentals and Applications, 2nd ed., Elsevier, 2015. https://doi.org/10.1016/S0927-5193(07)12021-0.

[4] M. La Cerva, L. Gurreri, M. Tedesco, A. Cipollina, M. Ciofalo, A. Tamburini, G. Micale, Determination of limiting current density and current efficiency in electrodialysis units, Desalination. 445 (2018) 138–148. https://doi.org/10.1016/j.desal.2018.07.028.

[5] W.Y. Shih, A. Rahardianto, R.W. Lee, Y. Cohen, Morphometric characterization of calcium sulfate dihydrate (gypsum) scale on reverse osmosis membranes, J. Memb. Sci. 252 (2005) 253–263. https://doi.org/10.1016/j.memsci.2004.12.023.

[6] A. American, N. Standard, Silt Density Index (SDI) of Water 1, Astm. 95 (2002) 7–9.

[7] R. Walker, Recent developments in ultrafiltration of electrocoat paint, Electrocoat. 82 (1982).

[8] Z. Wang, Z. Wu, G. Yu, J. Liu, Z. Zhou, Relationship between sludge characteristics and membrane flux determination in submerged membrane bioreactors, J. Memb. Sci. 284 (2006) 87–94. https://doi.org/10.1016/j.memsci.2006.07.006.

[9] C.R. Schulz, D.A. Okun, Treating surface waters for communities in developing countries, J. / Am. Water Work. Assoc. 75 (1983) 212–219. https://doi.org/10.1002/j.1551-8833.1983.tb05119.x.

[10] R. Endoh, T. Tanaka, M. Kurihara, K. Ikeda, New Polymeric Materials for Reverse Osmosis Membranes, Desalination. 21 (1977) 35–44. https://www.sciencedirect.com/science/article/abs/pii/S0011916400841077.

[11] A. Lopez, From Membranes to Mars, n.d.

[12] A.M. Lopez, M. Williams, M. Paiva, D. Demydov, T.D. Do, J.L. Fairey, Y.P.J. Lin, J.A. Hestekin, Potential of electrodialytic techniques in brackish desalination and recovery of industrial process water for reuse, Desalination. 409 (2017) 108–114. https://doi.org/10.1016/j.desal.2017.01.010.

[13] S. Kolahchyan, Ionic Liquid-Based Composite Thin-Films for Selective Ion Separations in Electrodialysis, University of Mississippi, 2019. https://egrove.olemiss.edu/cgi/viewcontent.cgi?article=2618&context=etd.

[14] R.W. Baker, Membrane Technology and Applications, 3rd ed., Wiley, 2012. https://doi.org/10.1016/s0958-2118(96)90133-0.

[15] C. Bartels, R. Franks, K. Andes, Operational Performance and Optimization of RO Wastewater Treatment Plants, Singapore Int. Water Week. 92058 (2010) 1–12. http://membranes.com/docs/papers/New Folder/Operational Performance and Optimization of RO Wastewater Treatment Plants.pdf.

[16] F. Valero, A. Barcelo, R. Arbos, Electrodialysis Technology; Theory and Applications, Mean F. Simul. Monte Carlo Integr. (2020) 85–124. https://doi.org/10.1201/b14924-7.

[17] mega, Antifreeze recycling; Ecological and effective solution of used ethylene glycol and propylene glycol disposal, (2021). https://www.mega.cz/antifreeze-recycling/.

[18] MEGA, Electrodialysis in dairy; Whey demineralization by MEGA electrodialysis applications, 2021. (n.d.). https://www.mega.cz/dairy-electrodialysis/.

[19] MEGA, Special Applications; RALEX standard and bipolar membrane electrodialysis for efficient production, separation and purification of your valuable substances, (2021). https://www.mega.cz/special/.

[20] M. Seko, H. Miyauchi, J. Omura, Ion Exchange Membranes: Principles, Production and Processes, 1986.

[21] GW Instek, GW Instek GPS Series Linear DC Power Supplies - Data Sheet, 2015. https://www.testequipmentdepot.com/instek/pdf/gps_data.pdf.

[22] A. Corporation, ASTOM Corporation Products Catalogue, 2017. http://www.astom-corp.jp/en/catalog/pdf/Astom_Products_Catalogue.pdf?20180213.

[23] Millipore Sigma, Direct-Q 3, 5, 8 Water Purification Systems, 2017.

[24] M. Chen, J. Ma, Z. Wang, X. Zhang, Z. Wu, Insights into iron induced fouling of ion-exchange membranes revealed by a quartz crystal microbalance with dissipation monitoring, RSC Adv. 7 (2017) 36555–36561. https://doi.org/10.1039/c7ra05510b.

[25] M.J. Edwards, Investigation of Fouling Mechanisms on Ion Exchange Membranes During Electrolytic Separations, The University of Mississippi, 2019.

[26] J.J. Krol, M. Wessling, H. Strathmann, Concentration polarization with monopolar ion exchange membranes: Current-voltage curves and water dissociation, J. Memb. Sci. 162 (1999) 145–154. https://doi.org/10.1016/S0376-7388(99)00133-7.

[27] D. Van Der Vliet, D.S. Strmcnik, C. Wang, V.R. Stamenkovic, N.M. Markovic, M.T.M. Koper, On the importance of correcting for the uncompensated Ohmic resistance in model experiments of the Oxygen Reduction Reaction, J. Electroanal. Chem. 647 (2010) 29–34. https://doi.org/10.1016/j.jelechem.2010.05.016.

APPENDIX

ED DATA

Neat NaCl	21-Jun	22-Jun	23-Jun		
Time (min)	Diluate (mS/cm)	Diluate (mS/cm)	Diluate (mS/cm)	AVG	STDEV
0	9.82	7.75	9.94	9.17	1.23
15	9.56	7.99	9.37	8.97	0.86
30	9.45	8.95	8.88	9.09	0.31
45	8.88	8.67	8.41	8.65	0.24
60	8.64	8.15	8.12	8.30	0.29
75	8.18	8.09	7.78	8.02	0.21
90	7.93	7.42	7.36	7.57	0.31
105	7.48	6.84	6.92	7.08	0.35
120	6.79	6.6	6.43	6.61	0.18
135	6.43	6.33	5.79	6.18	0.34
150	5.92	5.54	5.33	5.60	0.30
165	5.27	5.01	4.89	5.06	0.19
180	4.76	4.56	4.32	4.55	0.22

0.1 wt% SA	24-Jun	25-Jun	15-Jul		
Time (min)	Diluate (mS/cm)	Diluate (mS/cm)	Diluate (mS/cm)	AVG	STDEV
0	10.30	11.20	8.64	9.47	1.30
15	9.63	9.75	7.51	8.57	1.26
30	9.09	8.95	7.17	8.13	1.07
45	8.74	8.34	7.25	8.00	0.77
60	8.09	7.99	7.06	7.58	0.57
75	7.51	6.97	6.76	7.14	0.39
90	6.92	6.33	6.60	6.76	0.30
105	6.04	5.97	6.11	6.08	0.07
120	5.46	5.52	6.25	5.86	0.44
135	4.88	5.01	5.88	5.38	0.54
150	4.12	4.67	5.65	4.89	0.78
165	3.36	4.12	5.23	4.30	0.94
180	2.82	3.71	4.71	3.77	0.95

0.1 wt% BSA	28-Jun	29-Jun	16-Jul		
Time (min)	Diluate (mS/cm)	Diluate (mS/cm)	Diluate (mS/cm)	AVG	STDEV
0	9.19	8.61	9.02	9.11	0.30
15	8.28	7.75	8.24	8.26	0.30
30	7.84	8.02	7.87	7.86	0.10
45	7.63	7.51	8.02	7.83	0.27
60	7.22	7.25	7.87	7.55	0.37
75	6.92	7.36	7.22	7.07	0.22
90	6.23	6.71	6.55	6.39	0.24
105	6.21	6.43	6.02	6.12	0.21
120	5.42	6.11	5.23	5.33	0.46
135	5.37	5.81	4.27	4.82	0.79
150	4.55	5.54	3.94	4.25	0.81
165	4.25	5.27	3.43	3.84	0.92
180	3.97	5.11	2.87	3.42	1.12

0.25 wt% SA	2-July	6-Jul		
Time (min)	Diluate (mS/cm)	Diluate (mS/cm)	AVG	STDEV
0	8.31	8.28	8.30	0.02
15	6.71	7.42	7.07	0.50
30	6.28	7.11	6.70	0.59
45	6.06	6.73	6.40	0.47
60	5.37	6.43	5.90	0.75
75	4.91	6.04	5.48	0.80
90	4.56	5.74	5.15	0.83
105	4.29	5.59	4.94	0.92
120	3.94	5.25	4.60	0.93
135	3.57	4.93	4.25	0.96
150	3.23	4.82	4.03	1.12
165	3.08	4.55	3.82	1.04
180	2.82	4.76	3.79	1.37

0.25 wt% BSA	7-Jul	7-Jul		
Time (min)	Trial 1	Trial 2	AVG	STDEV
0	8.91	10.00	9.46	0.77
15	8.18	9.34	8.76	0.82
30	7.72	8.57	8.15	0.60
45	7.42	8.44	7.93	0.72
60	7.06	7.72	7.39	0.47
75	6.66	7.48	7.07	0.58
90	6.43	7.00	6.72	0.40
105	5.76	6.25	6.01	0.35
120	5.46	5.97	5.72	0.36
135	4.88	5.59	5.24	0.50
150	4.30	5.17	4.74	0.62
165	4.04	4.60	4.32	0.40
180	3.71	4.39	4.05	0.48

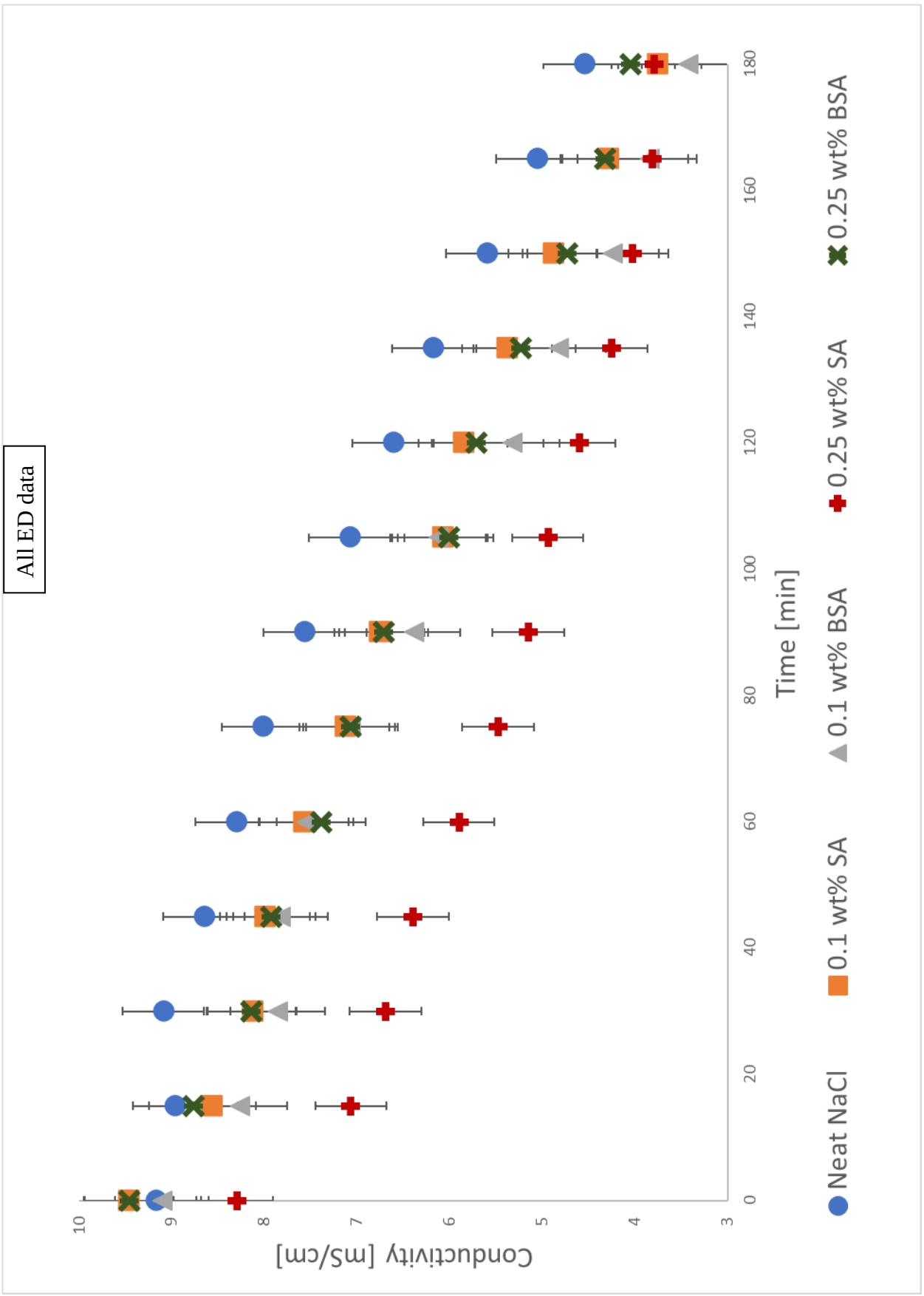
All ED data
Conductivity [mS/cm]
10
9
8
7
6
5
4
3
0
20
40
60
80
100
120
140
160
180
Time [min]
Neat NaCl
0.1 wt% SA
0.1 wt% BSA
0.25 wt% SA
0.25 wt% BSA

LCD DATA

Neat NaCl	Current Density (CD)	Current	CD^{-1}	Run 1		Run 2		
t [min]	I/A	I [A]	A/I]	V	Ω	V	Ω	AVG Ω
0		0		0.3		0.7		
5	1.72	0.01	0.5800	0.50	0.86	0.90	1.55	1.21
10	3.45	0.02	0.2900	0.80	2.76	1.10	3.79	3.28
15	5.17	0.03	0.1933	1.20	6.21	1.30	6.72	6.47
20	6.90	0.04	0.1450	1.70	11.72	1.50	10.34	11.03
25	8.62	0.05	0.1160	2.20	18.97	1.80	15.52	17.24
30	10.34	0.06	0.0967	2.50	25.86	2.10	21.72	23.79
35	12.07	0.07	0.0829	2.50	30.17	2.40	28.97	29.57
40	13.79	0.08	0.0725	3.00	41.38	2.70	37.24	39.31
45	15.52	0.09	0.0644	3.20	49.66	2.90	45.00	47.33
50	17.24	0.10	0.0580	3.30	56.90	3.00	51.72	54.31
55	18.97	0.11	0.0527	3.40	64.48	3.10	58.79	61.64
60	20.69	0.12	0.0483	3.60	74.48	3.30	68.28	71.38
65	22.41	0.13	0.0446	3.80	85.17	3.40	76.21	80.69
70	24.14	0.14	0.0414	4.10	98.97	3.50	84.48	91.72
75	25.86	0.15	0.0387	4.40	113.79	3.60	93.10	103.45
80	27.59	0.16	0.0363	4.40	121.38	3.70	102.07	111.72
85	29.31	0.17	0.0341	4.70	137.76	3.80	111.38	124.57
90	31.03	0.18	0.0322	4.80	148.97	4.00	124.14	136.55
95	32.76	0.19	0.0305	5.00	163.79	4.20	137.59	150.69
100	34.48	0.20	0.0290	5.10	175.86	4.50	155.17	165.52
105	36.21	0.21	0.0276	5.20	188.28	4.80	173.79	181.03
110	37.93	0.22	0.0264	5.40	204.83	5.00	189.66	197.24
115	39.66	0.23	0.0252	5.40	214.14	5.10	202.24	208.19
120	41.38	0.24	0.0242	5.60	231.72	5.10	211.03	221.38
125	43.10	0.25	0.0232	5.70	245.69	5.30	228.45	237.07
130	44.83	0.26	0.0223	5.80	260.00	5.40	242.07	251.03
135	46.55	0.27	0.0215	6.00	279.31	5.50	256.03	267.67
140	48.28	0.28	0.0207	6.10	294.48	5.70	275.17	284.83
145	50.00	0.29	0.0200	6.30	315.00	5.70	285.00	300.00
150	51.72	0.30	0.0193	6.30	325.86	5.90	305.17	315.52
155	53.45	0.31	0.0187	6.40	342.07	6.00	320.69	331.38
160	55.17	0.32	0.0181	6.50	358.62	6.00	331.03	344.83
165	56.90	0.33	0.0176	6.60	375.52	6.10	347.07	361.29
170	58.62	0.34	0.0171	6.80	398.62	6.20	363.45	381.03
175	60.34	0.35	0.0166	6.90	416.38	6.30	380.17	398.28
180	62.07	0.36	0.0161	7.00	434.48	6.40	397.24	415.86

0.0025 wt% Sodium Alginate Data

			16-Sep				23-Sep				26-Sep				27-Sep							
			run 1		run 2		run 1		run 2		run1		run2		run1		run2		run 3		AVERAGE	
t [min]	Amps	C.D.	V	Ω	V	Ω	V	Ω	V	Ω	V	Ω	V	Ω	V	Ω	V	Ω	V	Ω	V	Ω
0	0.00		0.90		1.00		0.20		0.80		0.60		1.10		0.80		1.00		1.00		0.91	
5	0.01	0.58	1.00	1.72	1.10	1.90	0.50	0.86	1.00	1.72	0.70	1.21	1.30	2.24	0.90	1.55	1.20	2.07	1.10	1.90	1.04	1.80
10	0.02	0.29	1.10	3.79	1.40	4.83	0.80	2.76	1.20	4.14	0.90	3.10	1.50	5.17	1.10	3.79	1.40	4.83	1.30	4.48	1.24	4.29
15	0.03	0.19	1.40	7.24	1.70	8.79	1.20	6.21	1.30	6.72	1.10	5.69	1.70	8.79	1.30	6.72	1.70	8.79	1.60	8.28	1.50	7.76
20	0.04	0.15	1.70	11.72	2.00	13.79	1.70	11.72	1.60	11.03	1.40	9.66	2.10	14.48	1.70	11.72	1.80	12.41	1.80	12.41	1.79	12.32
25	0.05	0.12	2.10	18.10	2.50	21.55	2.00	17.24	2.00	17.24	1.80	15.52	2.20	18.97	1.90	16.38	2.10	18.10	2.10	18.10	2.10	18.10
30	0.06	0.10	2.30	23.79	2.80	28.97	2.40	24.83	2.50	25.86	2.10	21.72	2.60	26.90	2.00	20.69	2.20	22.76	2.30	23.79	2.33	24.09
35	0.07	0.08	2.60	31.38	3.00	36.21	2.70	32.59	2.90	35.00	2.40	28.97	2.80	33.79	2.20	26.55	2.50	30.17	2.50	30.17	2.57	31.03
40	0.08	0.07	2.90	40.00	3.20	44.14	3.00	41.38	3.50	48.28	2.70	37.24	3.30	45.52	2.40	33.10	2.80	38.62	2.80	38.62	2.87	39.61
45	0.09	0.06	3.00	46.55	3.40	52.76	3.30	51.21	3.70	57.41	2.80	43.45	3.80	58.97	2.60	40.34	3.00	46.55	2.90	45.00	3.07	47.66
50	0.10	0.06	3.10	53.45	3.50	60.34	3.60	62.07	4.30	74.14	3.00	51.72	4.10	70.69	2.90	50.00	3.10	53.45	3.10	53.45	3.26	56.16
55	0.11	0.05	3.20	60.69	3.80	72.07	3.90	73.97	4.70	89.14	3.10	58.79	4.50	85.34	3.10	58.79	3.20	60.69	3.30	62.59	3.46	65.57
60	0.12	0.05	3.30	68.28	3.90	80.69	4.10	84.83	5.00	103.45	3.20	66.21	4.90	101.38	3.20	66.21	3.30	68.28	3.40	70.34	3.60	74.48
65	0.13	0.04	3.50	78.45	4.20	94.14	4.30	96.38	5.40	121.03	3.30	73.97	5.30	118.79	3.40	76.21	3.50	78.45	3.70	82.93	3.84	86.13
70	0.14	0.04	3.60	86.90	4.70	113.45	4.50	108.62	5.90	142.41	3.40	82.07	5.60	135.17	3.70	89.31	3.60	86.90	3.90	94.14	4.07	98.28
75	0.15	0.04	3.70	95.69	5.10	131.90	4.90	126.72	6.10	157.76	3.50	90.52	6.00	155.17	3.90	100.86	3.80	98.28	4.20	108.62	4.31	111.58
80	0.16	0.04	3.90	107.59	5.30	146.21	5.00	137.93	6.50	179.31	3.70	102.07	6.20	171.03	4.10	113.10	4.00	110.34	4.40	121.38	4.51	124.53
85	0.17	0.03	4.00	117.24	5.60	164.14	5.30	155.34	6.80	199.31	3.90	114.31	6.50	190.52	4.40	128.97	4.20	123.10	4.80	140.69	4.77	139.85
90	0.18	0.03	4.20	130.34	5.80	180.00	5.40	167.59	6.90	214.14	4.00	124.14	7.00	217.24	4.80	148.97	4.50	139.66	5.00	155.17	5.04	156.50
95	0.19	0.03	4.30	140.86	5.90	193.28	5.50	180.17	7.30	239.14	4.10	134.31	7.40	242.41	5.20	170.34	4.80	157.24	5.40	176.90	5.30	173.62
100	0.20	0.03	4.60	158.62	6.10	210.34	5.80	200.00	7.60	262.07	4.30	148.28	7.80	268.97	5.60	193.10	5.20	179.31	5.80	200.00	5.63	194.09
105	0.21	0.03	4.90	177.41	6.20	224.48	5.90	213.62	7.90	286.03	4.40	159.31	8.00	289.66	5.80	210.00	5.20	188.28	6.00	217.24	5.79	209.48
110	0.22	0.03	5.20	197.24	6.40	242.76	6.30	238.97	8.40	318.62	4.50	170.69	8.50	322.41	6.10	231.38	5.30	201.03	6.30	238.97	6.04	229.21
115	0.23	0.03	5.30	210.17	6.50	257.76	6.40	253.79	8.70	345.00	4.50	178.45	8.60	341.03	6.30	249.83	5.40	214.14	6.60	261.72	6.17	244.73
120	0.24	0.02	5.40	223.45	6.60	273.10	6.50	268.97	8.90	368.28	4.60	190.34	8.90	368.28	6.40	264.83	5.50	227.59	6.80	281.38	6.31	261.28
125	0.25	0.02	5.50	237.07	6.90	297.41	6.70	288.79	9.30	400.86	4.80	206.90	9.00	387.93	6.70	288.79	5.60	241.38	7.10	306.03	6.51	280.79
130	0.26	0.02	5.70	255.52	7.00	313.79	6.90	309.31	9.40	421.38	4.90	219.66	9.10	407.93	6.80	304.83	5.60	251.03	7.20	322.76	6.61	296.50
135	0.27	0.02	5.70	265.34	7.10	330.52	7.00	325.86	9.60	446.90	5.00	232.76	9.30	432.93	7.40	344.48	5.80	270.00	7.40	344.48	6.81	317.22
140	0.28	0.02	5.90	284.83	7.30	352.41	7.30	352.41	9.70	468.28	5.10	246.21	9.40	453.79	7.80	376.55	5.90	284.83	7.60	366.90	7.00	337.93
145	0.29	0.02	6.00	300.00	7.50	375.00	7.50	375.00	10.10	505.00	5.20	260.00	9.70	485.00	7.90	395.00	6.00	300.00	7.70	385.00	7.14	357.14
150	0.30	0.02	6.20	320.69	7.70	398.28	7.80	403.45	10.30	532.76	5.30	274.14	9.90	512.07	8.10	418.97	6.10	315.52	7.90	408.62	7.31	378.33
155	0.31	0.02	6.20	331.38							5.40	288.62	10.00	534.48							7.20	384.83
160	0.32	0.02	6.20	342.07							5.50	303.45	10.10	557.24							7.27	400.92
165	0.33	0.02	6.30	358.45							5.50	312.93	10.30	586.03							7.37	419.14
170	0.34	0.02	6.40	375.17							5.70	334.14	10.40	609.66							7.50	439.66
175	0.35	0.02									5.80	350.00	10.50	633.62							8.15	491.81
180	0.36	0.02									5.80	360.00	10.70	664.14							8.25	512.07
185	0.37	0.02									5.90	376.38	10.90	695.34							8.40	535.86
190	0.38	0.02									6.00	393.10	11.10	727.24							8.55	560.17
195	0.39	0.01									6.10	410.17	11.20	753.10							8.65	581.64
200	0.40	0.01									6.20	427.59	11.40	786.21							8.80	606.90

VITA

EDUCATION

2015-2018 B.S. Professional Chemistry with Applied Mathematics, Kennesaw State University

2010-2012 B.B.A. Marketing, North Georgia College and State University